J Mater Sci (2007) 42:2297–2303
DOI 10.1007/s10853-006-0601-y

4TH BRAZILIAN MRS MEETING

Superparamagnetic relaxation evidences large surface contribution for the magnetic anisotropy of $MnFe_20_4$ nanoparticles of ferrofluids

C. R. Alves · Renata Aquino · Jérôme Depeyrot · Francisco A. Tourinho · Emmanuelle Dubois · Régine Perzynski

Received: 8 November 2005 / Accepted: 20 June 2006 / Published online: 27 February 2007

Abstract Manganese ferrite nanoparticles, in the size range 3.3–9.0 nm, are prepared by a hydrothermal coprecipitation process and peptized in aqueous solution. The magnetization curves recorded at room temperature on diluted colloidal sols allow characterizing the distribution of magnetic moment by using a simple Langevin formalism. Mössbauer spectroscopy measurements performed on powder samples at 77 K exhibit a quadrupolar doublet which intensity grows at the expense of the hyperfine sextet pattern as the nanoparticles mean size decreases. The magnetic dynamics behavior is then investigated by measurements of magnetic hysteretic properties at 5 K and temperature dependence of the zero field cooling (ZFC) susceptibility. The values found for the effective anisotropy constant and the dependence of the irreversibility field, inversely proportional to the reference size, clearly indicate that the magnetic anisotropy of our nanoparticles finds its origin on the disordered surface layer.

C. R. Alves · R. Aquino · J. Depeyrot (✉)
Complex Fluid Group, Instituto de Física, Universidade de Brasília, CP 04455, Brasília, DF 70919-970, Brazil
e-mail: depeyrot@fis.unb.br

F. A. Tourinho
Complex Fluid Group, Instituto de Química, Universidade de Brasília, CP 04478, Brasília, DF 70919-970, Brazil

R. Aquino · E. Dubois · R. Perzynski
Laboratoire des Liquides Ioniques et Interfaces Chargées, Université Pierre et Marie Curie, Bât. F, Case 63, 4 place Jussieu, Paris Cedex 05 75252, France

Introduction

Magnetic properties of nanosized ferrites particles are a subject of great interest from both technological and theoretical research [1, 2]. When dispersed in a liquid carrier at room temperature, it leads to magnetic liquids, which are widely used in technological devices applications such as sensors of acceleration or pressure, in assisted shock absorbers or magneto-optical modulators [3, 4]. Magnetic nanoparticles are also currently very promising materials for the design of new magneto-pharmaceuticals [5]. When dispersed in a complex medium like a gel, a liquid crystal, or a biological cell, they can behave as nanoscaled magnetic probes in order to investigate the local rheological properties of the medium carrier [6]. When dispersed in a solid matrix, their interest essentially lies in their use in ultra-high density magnetic information storage [1]. From a more fundamental point of view, these applications require the knowledge of how the properties of magnetic systems differ from bulk ones when the size decreases to the nanometric range [7]. Indeed, the reduction of particle size at nanoscale leads to a complex interplay, between finite-size and interface effects, which is responsible for the magnetic behavior of nanoparticles and enhanced as the particle size decreases. The reduced symmetry of surface atoms, which have a nearest neighbor on one side and none on the other side, does induce a large number of broken exchange bonds and can result in surface anisotropy, frustration and spin disorder [2].

With the reduction of the particle size at nanoscale, the surface to volume ratio becomes very large and enhanced surface anisotropy is expected. If several theoretical approaches exists [2, 8, 9], nevertheless, little work has been done with ferrite nanoparticles to

investigate experimentally the surface contribution to the total anisotropy. Very recently, low temperature magnetization and AC susceptibility measurements have shown that the anisotropy of maghemite nanoparticles systems [10] is induced by the particle surface. Such results are in good agreement with those obtained by ferromagnetic resonance experiments performed on γ-Fe_2O_3 nanoparticles of ferrofluids [11]. A systematic experimental determination of the anisotropy energy or field as a function of the size of the nanoparticle would allow, by tuning the surface to volume ratio, to establish the size scaling laws for these properties [7].

In this work, we investigate the magneto-dynamic properties of manganese spinel ferrite nanoparticles of Electric Double Layered Magnetic Fluids (EDL-MF). Very recently, it has been analyzed in details the thermal and nanoparticle size dependences of the high field magnetization of colloidal dispersions of such nanoparticles [12]. The thermal variations of magnetization are interpreted in terms of a modified Bloch law, accounting for finite size effect, and an extra surface contribution, corresponding to surface spins misaligned with those of the ordered core, which freezes in a disordered structure at temperatures lower than 70 K. In the present paper, before detailing our experimental results, we present a theoretical background which seems to us essential in order to make easier the understanding of this work. Then we show how our measurements point the main role played by surface spins in the thermal activated relaxation and in high field irreversibility.

Experimental section

Particle synthesis and magnetic fluid elaboration

The EDL-MF preparation is carried out using a hydrothermal coprecipitating aqueous solution of a $MnCl_2$–$FeCl_3$ mixture in alkaline medium [13, 14]. After the coprecipitation step, the precipitate is washed in order to reduce the high ionic strength of the medium and the particle surface is cleaned by a HNO_3 solution (2 mol L^{-1}). Moreover, to ensure the thermodynamical stability of the particles an empirical process is used: the precipitates are boiled with a 0.5 mol L^{-1} $Fe(NO_3)_3$ solution. Then, the particles are conveniently peptized in an acidic medium by adjustment of the ionic strength, resulting in a stable sol of high quality. $MnFe_2O_4$ nanoparticles with different mean sizes have been obtained by monitoring the hydroxide concentration during the coprecipitation step of the ferrofluid chemical synthesis [15].

Synthesis characterization

In order to determine the samples composition, suitable chemical titrations are performed. Iron (III) titration is performed by dichromatometry and the manganese (II) concentration is determined using inductively coupled plasma atomic emission spectroscopy (ICP-AES). Table 1 lists the volume fraction ϕ in magnetic nanomaterial of all the samples investigated in this work.

X-ray diffraction (XRD) measurements

In order to determine the nanocrystal size and structures, XRD spectra are recorded from powder samples obtained by evaporation of the liquid carrier and by using a diffractometer installed in a conventional Rigaku-Denki generator operating at 40 kV/20 mA and the CuKα radiation monochromatized by a graphite monochromator.

Transmission electron microscopy (TEM)

In order to obtain the size distribution of our nanoparticles, electron microscopy measurements were performed on a Transmission Electronic Microscope JEOL 100CX2, after evaporation of a very dilute fluid sample.

Mössbauer measurements

Mössbauer absorption spectra were performed at 77 K using a conventional constant-acceleration

Table 1 Sample characteristics: d_{XR} is the mean size calculated from X ray powder diffractogram, d_0 is the TEM characteristic diameter, s_d is the TEM polydispersity index, ϕ is the volume fraction of magnetic material, μ is the mean magnetic moment of the nanoparticles, s_μ is the polydispersity index, $\gamma^{300°K}$ is the parameter of dipolar interaction at 300 K, M_{max}/ϕ is the normalized magnetization of the liquid solution and m_s is the magnetization of the nanomaterial at 300 K obtained from the fit with a Langevin formalism

Sample	d_{XR} (nm)	d_0 (nm)	s_d	ϕ^{eff}%	$<\mu>$ ($10^3\mu_B$)	s_μ	$\gamma^{300\ K}$	M_{max}/ϕ (kA/m)	m_s (kA/m)
QMn2	9	8	0.25	0.45	17.2	1.2	0.32	370	375
QMn1	7.4	6.4	0.27	1.54	6.5	1.3	0.36	280	285
QMn4	4.2	3.3	0.3	0.45	3.3	1.4	0.08	242	250
QMn3	3.3	2.8	0.3	0.45	1.1	1.2	0.01	117	130

spectrometer in transmission geometry with a source of about 50 mCi ^{57}Co in a Rh matrix, on powder samples.

Magnetic measurements

The superconducting-quantum-interference-device (SQUID) magnetometer from GPS—UPMC—France is used to perform magnetic measurements for all MF samples between 5 K and 300 K. The hysteresis loops were recorded at 5 K in a magnetic field H range—4×10^3 kA/m < H < 4×10^3 kA/m. In our experiments, the carrier medium is aqueous so that below 273 K it becomes solid. If the freezing process is sufficiently rapid, the magnetic solution maintains the same state of particle dispersion than at room temperature. Moreover, measurements as a function of the temperature were realized. In this case, after the ZFC process, a field of 30 Oe is applied and the variation of the susceptibility is measured with increasing temperature.

Results and discussion

A typical powder diffractogram is shown in Fig. 1 and exhibits several lines corresponding to the characteristic interplanar spacing 220, 311, 400, 422, 511 and 440 of the spinel structure. The size of the cubic cell is found equal to 0.840 nm to be compared with the ASTM value equal to 0.849 nm for $MnFe_2O_4$ bulk material. According to the Scherrer equation, the nanoparticle size d_{XR} is related to the broadening of the diffracted beam and the values, calculated using the most intense peak, are collected in Table 1. The inset of Fig. 1 presents the TEM picture obtained for the same sample and shows that the particles are roughly spherical. The size histogram is obtained from a statistic over 500 particles and well adjusted with a log-normal distribution law, well described by an average diameter d_0 and a size dispersion index s_d (polydispersity). Table 1 presents the values of d_{XR}, d_0 and s_d obtained for all samples, using the same described procedure and both determinations well compare using $d_{XR} = d_0 e^{2.5 s_d^2}$ [16].

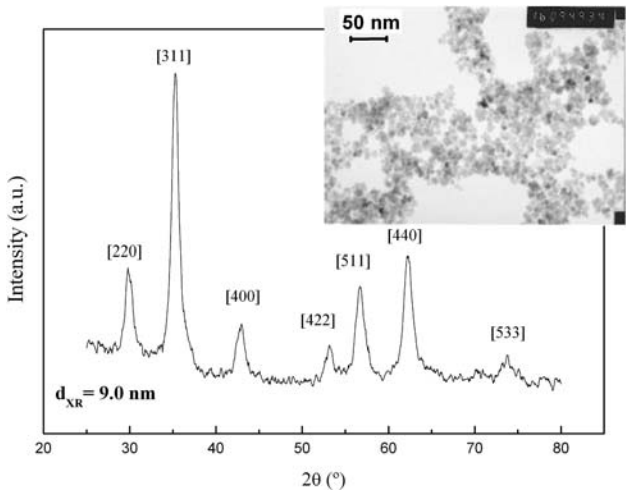

Fig. 1 X-ray powder diffractogram of QMn2 sample. The characteristic [hkl] interplanar planes of spinel structure are labeled. The inset displays a TEM picture for the same sample

Diluted magnetic colloidal solutions offer the possibility to investigate the magnetic behavior of a single magnetic nanoparticle since they constitute an ensemble of non interacting magnetic moments [17] $\mu = m_S V$, m_S being the saturation magnetization of the nanomaterial and V the particle volume. However, such nanomaterials present a moment distribution that can be well characterized by magnetization measurements performed at room temperature. Indeed, the magnetic fluid response to an applied field H results from the progressive orientation in the field of the magnetic moments of the distribution which are free to rotate in the solvent. This superparamagnetic behavior is therefore well described by the Langevin formalism including a log-normal distribution of magnetic moments [12]:

$$Q(\mu) = \frac{1}{\sqrt{2\pi}\mu s_\mu} \exp\left[-\frac{\ln^2\left(\mu/\mu^0\right)}{2 s_\mu^2} \right], \quad (1)$$

where s_μ is the polydispersity index (by definition $s_\mu = 3 s_d$) of $\ln\mu$ and $\ln\mu^0 = \langle \ln\mu \rangle$. Then, the magnetization of the colloidal solution is a superposition of the contribution of each individual particle weighted by the distribution of magnetic moments and writes:

$$\frac{M}{m_S \phi} = \frac{\int L\left[\xi(\mu, s_\mu)\right] Q(\mu) d\mu}{\int Q(\mu) d\mu}, \quad (2)$$

where $\xi = \mu_0 \mu H / k_B T$ and $L(\xi) = \coth\xi - 1/\xi$ are respectively the Langevin parameter and the Langevin function. At low field, $\xi << 1$, the initial magnetic susceptibility can be related to the dipolar interaction parameter γ using Eq. (2):

$$\chi_0 = \frac{M}{H} = \frac{m_S \phi \mu_0 \mu}{3 k_B T} = \frac{\gamma}{3}. \quad (3)$$

In the following, we will begin by analyzing such room temperature magnetization curves in order to show that our investigated magnetic colloids samples

are diluted enough to be considered as a gas of independent particles, and to determine the parameters of the magnetic moment distribution. Then, Mössbauer spectroscopy and magnetic measurements at low temperatures allow us to investigate the Néel superparamagnetic relaxation of our $MnFe_2O_4$ nanoparticles.

Figure 2 displays a typical experimental magnetization curve obtained at room temperature for sample QMn2. The magnetization is zero in the absence of an external field, is also an increasing function of the applied field and saturates at 4×10^3 kA/m, in good qualitative agreement with the Langevin model. All these observations are similar for all samples excepted for the sample QMn3, based on smaller mean size, which presents a magnetization not fully saturated at large field. The inset of Fig. 2 presents for all the samples low field measurements and the slope of the straight line gives the initial susceptibility, thus providing an experimental estimate of the dipolar interaction parameter. The γ values found here (see Table 1) are always lower than 1, a result which indicates [18] that the magnetic particle-particle interactions are negligible for all the volume fractions in magnetic nanoparticle of Table 1, justifying, for all our samples, the use of an independent particle model. In this context, the full line in Fig. 2 is the curve obtained by fitting the experimental data to Eq. 2 using a Fortran numerical routine, based on the least square method, that allows to determine m_S, μ^0 and s_μ. The values of these parameters, of the deduced mean magnetic moment $\langle\mu\rangle = \mu^0 e^{-0.5 s_\mu^2}$ and of the normalized magnetization of the liquid solution $M_{\max}/\phi$, at $T = 300$ K and $H = 4 \times 10^3$ kA/m, are listed, for each sample, in Table 1. In all the cases, the robustness of the fitted parameters values is ensured by a typical correlation coefficient around 0.998. The values of s_μ indicate a large moment distribution and show little discrepancy with those of s_d since the experimental determination of both polydispersity indexes are obtained by using different experimental techniques. Table 1 also indicates that the magnetization (both m_S and $M_{\max}/\phi$) is largely reduced as the nanoparticle size decreases, a result which can be attributed to finite-size effect of the magnetic core [12]. Moreover, analyzing the difference between both values shows that, at 4×10^3 kA/m, the magnetization of samples based on larger nanoparticles is close to saturation when compared to sample QMn3, based on smallest particles, presenting a magnetization not fully saturated.

Figure 3 shows the Mössbauer spectra of powder samples recorded at 77 K after evaporation of the liquid solution. As the nanoparticles mean size

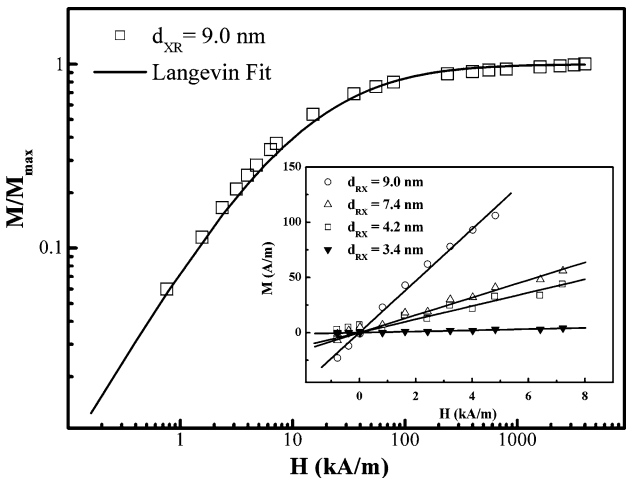

Fig. 2 Normalized room temperature magnetization curve for QMn2 sample; the full line is the best Langevin adjust. The inset displays the initial magnetic susceptibility for all samples; the full line is a linear fit

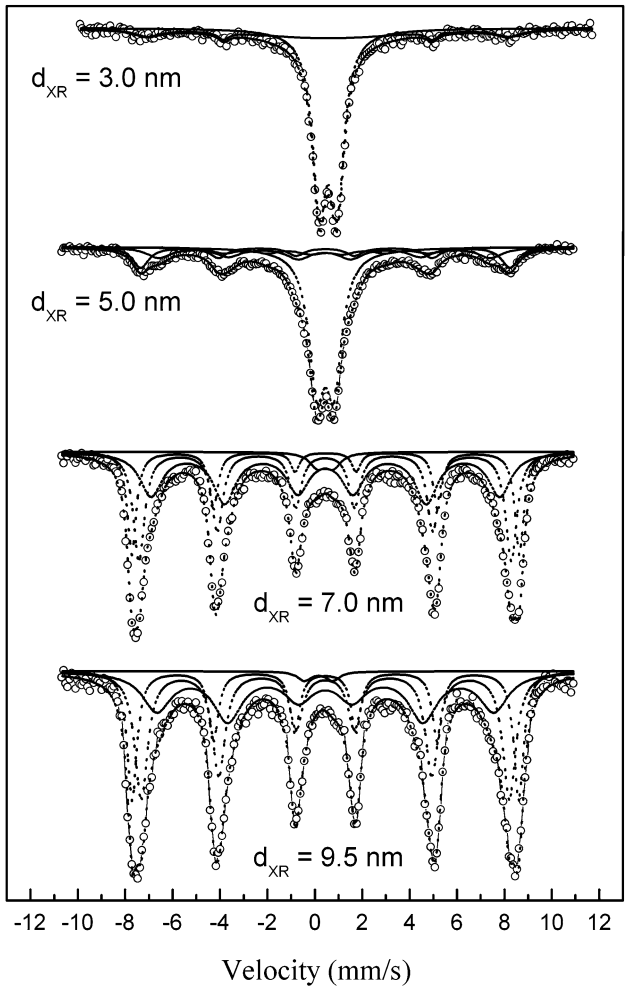

Fig. 3 77 K Mössbauer spectra fitted with three hyperfine sextets and one doublet, the exception is the sample with $d_{XR} = 3.3$ nm which was fitted with one sextet and one doublet

decreases, the presence of a doublet, which intensity grows at the expense of the sextet, can be observed. This behavior is typical [19] of superparamagnetic relaxation and can be enlightened considering two populations: one based on large particles, which fluctuate slowly (larger anisotropy energy), giving rise to the hyperfine sextet and one other, based on smaller particles (smaller anisotropy energy) with shorter relaxation time, yielding a quadrupolar doublet [20]. A simple approach to fit these spectra provides a qualitative analysis of the magnetic behavior of our nanoparticles. The spectra corresponding to sample QMn3 (d_{XR} = 3.3 nm) is well accounted by considering a superposition of a hyperfine field distribution and a quadrupolar doublet, due to superparamagnetic particles, as already reported for 3 nm sized cobalt ferrite nanoparticles [20]. The intensity of the doublet is much larger than the sextet showing that most of the magnetic moments are not blocked a result due to the very small size of these nanoparticles. All others spectra can be fitted using three sextets, two associated to the well magnetically ordered core and corresponding to Fe^{3+} atoms at tetrahedral and octahedral site in the spinel structure and a third sextet attributed to a surface shell of disordered spins as a consequence of the incomplete and distorted atomic surrounding at the nanoparticle surface. Indeed, it has been shown, by in field Mössbauer spectroscopy measurements performed at 4.2 K with nickel [21] and copper [22] ferrite nanoparticles of ferrofluids, that a fraction of the spins remains canted with regard to the direction of the applied field. This fraction of misaligned spins increases as the nanocrystal size decreases showing that these spins are those of the surface of the nanoparticles. Moreover, to achieve the fit of the spectra corresponding to samples QMn4 (d_{XR} = 4.2 nm), QMn1 (d_{XR} = 7.4 nm) and QMn2 (d_{XR} = 9.0 nm) the doublet, characteristic of superparamagnetic particles, has also to be included. This result shows that, even for samples based on large nanoparticles (mean size between 7.4 and 9 nm), a non zero fraction of magnetic moments, associated with the smaller particles of the log-normal size distribution, are already fluctuating at T = 77 K. The Mössbauer parameters deduced from the fitting procedure are given in Table 2. The sextet with the largest hyperfine field value is associated to iron ions located at octahedral sites (B sites) of the spinel-type nanostructure and the sextet with the smallest isomer shift value corresponds to iron ions at tetrahedral sites (A sites) [23]. The third broad sextet S presents the smallest hyperfine field value and is related with disordered surface spins. Table 2 also shows that decreasing the particle size yields a reduction of the hyperfine field value in good accordance with the model of collective magnetic excitations [24].

Figure 4(a, b) display the temperature dependence of the susceptibility in the case of ferrofluid sample QMn1 at two different volume fractions and in the case of diluted colloidal solution based on our size-controlled $MnFe_2O_4$ nanoparticles (see the volume fraction of the diluted sols in Table 3). Let us, first, qualitatively comment both Figures which clearly illustrate the superparamagnetic behavior of the investigated nanoparticles. Indeed, when an ensemble of individual particles is frozen without applied field, the magnetic moments are randomly oriented and the resulting magnetization is zero. With increasing temperature, the magnetic moments can fluctuate and then align in the direction of the very low field applied, leading to an increase of the total magnetization. Above the Blocking temperature, superparamagnetic behavior sets in, leading to a decrease of the total magnetization. The presence of a maximum in the ZFC susceptibility curve is therefore associated to the transition between superparamagnetic and blocked behavior. Moreover, the transition is not sharp as a

Table 2 Mössbauer parameters at 77 K for our Manganese ferrite nanoparticles, H_{hyp} is the hyperfine field, IS the isomer shift, QS the quadrupole splitting and Γthe line width

Sample		H_{hyp} (kOe)	IS (mm/s)	QS (mm/s)	Γ (mm/s)
QMn2	*Doublet*	–	0.45	0.71	0.695
	A	488	0.441	0.02	0.662
	B	507	0.45	0.04	0.492
	S	443	0.444	0.015	1.443
QMn1	*Doublet*	–	0.444	0.673	0.784
	A	483	0.435	0.035	0.574
	B	506	0.457	0.02	0.445
	S	457	0.448	0.025	1.128
QMn4	*Doublet*	–	0.446	0.726	0.815
	A	435	0.414	0.015	1.235
	B	484	0.442	0.008	0.844
	S	268	0.486	0.02	1.236
QMn3	*Doublet*	–	0.44	0.744	0.714
	Sextet	473	0.45	0.035	2.2

The center shifts are corrected to ±0.01 mm/s, quadrupole splitting to ±0.02 mm/s, and the hyperfine magnetic fields are corrected to ±1 kOe

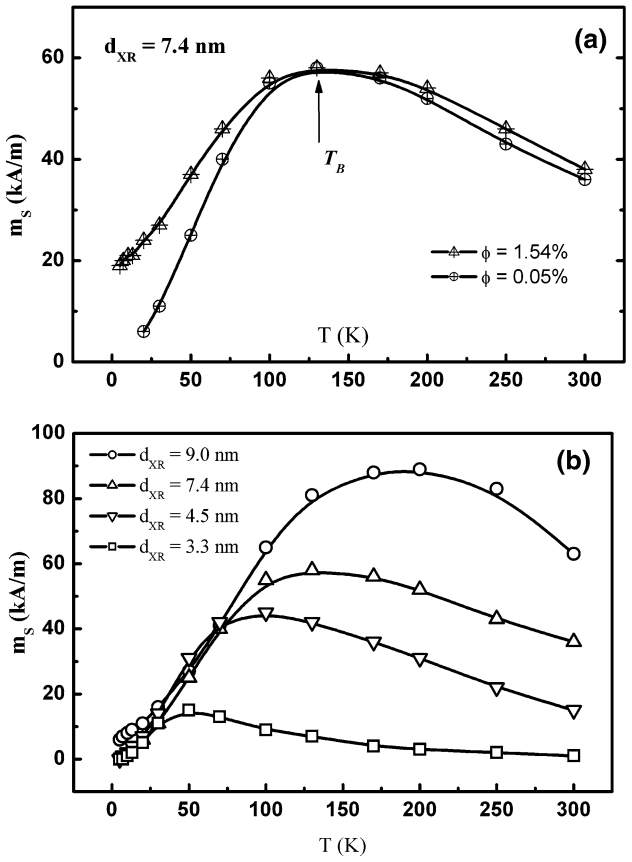

Fig. 4 ZFC curves in applied field of 2.4 kA/m. (**a**) Obtained curve for different values of dipolar interaction parameters (the arrow points the blocking temperature). (**b**) Blocking temperature evolution with particle size

consequence of the size distribution. Figure 4(a) indicates that when the volume fraction of sample QMn1 varies about 40 times from 0.05% to 1.54% the blocking temperature is the same showing that in this range, the magnetic dynamics of the colloidal solution remains governed by the dynamics of isolated magnetic nanoparticles. Figure 4(b) evidences that as the nanocrystal mean size increases, the Blocking temperature is shifted towards higher temperatures, reflecting as expected, larger anisotropy energy.

Table 3 lists the values of the measured Blocking temperature and the deduced anisotropy energy.

Table 3 Blocking temperature T_B, anisotropy energy E_A, effective constant K_{eff}, deduced from temperature dependence of susceptibility measurements, and the value of the irreversible field H_{irr} determined from the hysteresis loop

Sample	ϕ (%)	T_B (°K)	E_A (J)	K_{eff} (J/m^3)	H_{irr} (Oe)
QMn2	0.01	200	6.50E–20	1.70E+05	2.98
QMn1	0.05	130	4.23E–20	2.00E+05	5
QMn4	0.07	100	3.25E–20	8.40E+05	6.5
QMn3	0.045	50	1.63E–20	8.70E+05	9.98

Table 3 also presents the values of the effective magnetic anisotropy constant K_{eff}, extracted from the total energy anisotropy, proportional to the particle volume, by using the average particle diameter from X ray diffraction data listed in Table 1. One can note the large values of K_{eff} deduced here, especially when compared to the first-order magneto-crystalline anisotropy constant of bulk $MnFe_2O_4$, equal to 4.0×10^3 J m^{-3} [25]. The two order of magnitude difference between both determinations and the increase of the effective value with decreasing size denote the surface anisotropy domination in the magnetic dynamics of our nanoparticles. The average value of the resulting surface constant $K_S = K_{eff}d/6$, d being the particle diameter is about 3.9×10^{-4} J m^{-2}, comparable with the values found for maghemite [11] and nickel ferrite [21] nanoparticles of similar mean sizes obtained by using the same chemical synthesis.

We propose now to analyze at 5 K the size dependence of the field H_{irr} under which the hysteresis cycle $M \times H$ is irreversible (loop closure). In Fig. 5, H_{irr} is plotted in a double logarithmic representation as a function of the nanocrystal size d_{XR}. The inset displays the typical opened hysteresis loop measured at 5 K for sample QMn3 where the arrow indicates the irreversible field. The value of H_{irr} between 3 kOe and 10 kOe, is in good agreement with high closure fields in the hysteresis loops obtained for nickel ferrite nanoparticles [26]. In double logarithmic plot, a fit performed using a d^{α} law should give a straight line of slope α. The full line in Fig. 5 corresponds to the best fit and leads to $\alpha \approx -1$, showing therefore that the irreversibility field is inversely proportional to the reference size, a result

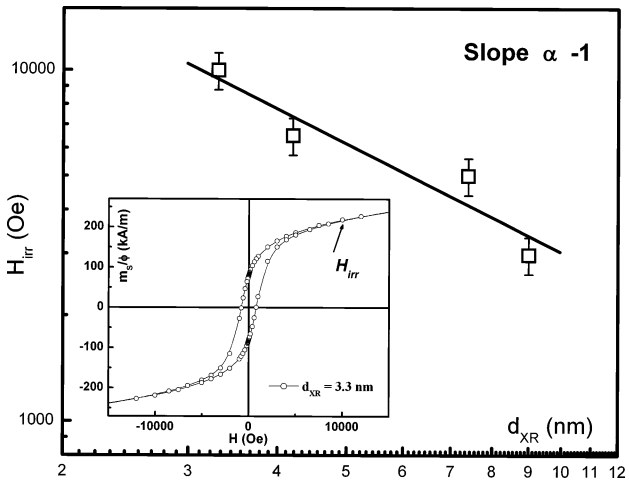

Fig. 5 Double Logarithmic representations of the irreversible field with the particle mean size at 5 K. The inset displays a detail of a hysteresis loop indicating the determination of H_{irr}

which indicates surface-related phenomena. Indeed, the irreversibility field well compares with the effective internal field or anisotropy field H_A, which maintains the magnetic moment in the easy magnetization direction [10]. Then, if one writes the magnetic anisotropy energy of a particle as a surface contribution, H_{irr} only can scale with $1/d$. The dependence of the effective internal field on the inverse reference size is a fingerprint of the surface anisotropy domination in the magnetic dynamics properties [7].

Summary

Using a soft chemical route, we successfully synthesized manganese ferrite nanoparticles of controlled average size ranging between 3 nm and 9 nm. Magnetization measurements have shown that the magnetic properties at 300 K are well described by a single domain configuration and a simple Langevin model leads to the magnetic moments distribution.

Mössbauer spectroscopy measurements performed at 77 K, as a function of the particle size, indicate typical superparamagnetic behavior and a model of two populations, one based on magnetic moments which fluctuate slowly and one other based on magnetic moments which relax more rapidly, allow fitting the spectra.

Our experimental determination of the single-domain anisotropy energy and the irreversibility field of manganese ferrite nanoparticles have provided direct evidence for the importance of surface effects for the magnetic behavior at the nanometric size scale. The effective magnetic anisotropy constant K_{eff}, extracted from the total energy anisotropy, proportional to the particle volume, is two order of magnitude larger than the bulk value. The effective internal field which maintains the magnetic moment blocked in the easy direction well scale with $1/d$, showing unambiguously an enhanced surface contribution for the magnetic anisotropy.

Acknowledgments The authors are greatly indebted to L. Legrand, from the Groupe de Physique des Solides of Université Paris 6, which allows us to perform our magnetization measurements using a SQUID magnetometer. This work was supported by the Brazilian agencies Finatec, CNPq and CAPES through the contract of international cooperation CAPES/ COFECUB no. 496/05.

References

1. Batle X, Labarta A (2002) J Phys D Appl Phys 35:R15
2. Kodama RH (1999) J Magn Magn Mat 200:359
3. Berkovsky B (1996) Magnetic fluids and applications – Handbook. Begell House, New York, p 36
4. Rosensweig R (1985) Ferrohydrodynamics. Cambridge University Press, Cambridge
5. Deux JF, Riviere C, Gazeau F, Roger J, Allaire E, Boudghene F, Michel JB, Letourneur D (2003) Circulation 108:2497
6. Wilhelm C, Gazeau F, Roger J, Pons JN, Salis MF, Perzynski R, Bacri JC (2002) Phys Rev E 66:021203
7. Raikher YUL, Perzynski R (2005) In: D. Fiorani (ed) Surface effects in magnetic nanoparticles. Springer Publ., New York
8. Garanin DA, Kachkachi H (2003) Phys Rev Lett 90:065504
9. Iglesias O, Labarta A (2005) J Magn Magn Mater 290–291:738
10. Fiorani D, Testa AM, Lucari F, D'orazio F, Romero H (2002) Physica B 320:122
11. Gazeau F, Bacri JC, Gendron F, Perzynski R, Raikher YUL, Stepanov VI, Dubois E (1998) J Magn Magn Mater 186:175
12. Aquino R, Depeyrot J, Sousa MH, Tourinho FA, Dubois E, Perzynski R (2005) Phys Rev B 72:184435
13. Tourinho FA, Franck R, Massart R (1990) J Mater Sci 25:3249
14. Sousa MH, Tourinho FA, Depeyrot J, Da Silva GJ, Lara MCFL (2001) J Phys Chem B 105:1168
15. Aquino R, Tourinho FA, Itri R, Lara MCFL, Depeyrot J (2002) J Magn Magn Mater 252:23
16. Tronc E, Bonnin D (1985) J Phys Lett 46:L437
17. Cousin F, Dubois E, Cabuil V (2003) Phys Rev E 68:021405
18. Gazeau F, Boué F, Dubois E, Perzynski R (2003) J Phys Cond. Mat 15:S1305
19. Mørup S, Dumesic JA, Topsøe H (1980) In: L. R. Chen (ed) Applications of Mössbauer pectroscopy, vol. II. Academic Press, New York, p 1
20. Moumen N, Bonville P, Pileni MP (1996) J Phys Chem 100:14410
21. Sousa EC, Sousa MH, Goya GF, Rechenberg HR, Lara MCFL, Tourinho FA, Depeyrot J (2004) J Magn Magn Mater 272:1215
22. Alves CR, Sousa MH, Aquino R, Rechenberg HR, Goya GF, Tourinho FA, Depeyrot J (2004) J Metastable Nanocryst Mat 21:17
23. Chinnasamy CN, Narayanasamy A, Ponpandian N, Chatttopadhyay K, Shinoda K, Jeyadevan B, Tohji K, Nakatsuka N, Furubayashi T, Nakatani I (2001) Phys Rev B 63:184108
24. Mørup S (1983) J Magn Magn Mater 37:39
25. Cullity BD (1972) Introduction to magnetic materials. Addison Wesley, New York
26. Kodama RH, Berkowitz AE (1999) Phys Rev B 59:6321